

Available online at [www.sciencedirect.com](http://www.sciencedirect.com)**SciVerse ScienceDirect**

Energy Procedia 00 (2013) 000–000

**Energy  
Procedia**[www.elsevier.com/locate/procedia](http://www.elsevier.com/locate/procedia)

European Geosciences Union General Assembly 2013, EGU

Division Energy, Resources &amp; the Environment, ERE

## 3D hydro-mechanical scenario analysis to evaluate changes of the recent stress field as a result of geological CO<sub>2</sub> storage

Fabien Magri<sup>a,\*</sup>, Elena Tillner<sup>a</sup>, Wenquing Wang<sup>b</sup>, Norihiro Watanabe<sup>b</sup>,  
Günter Zimmermann<sup>a</sup>, Thomas Kempka<sup>a</sup>

<sup>a</sup>GFZ German Research Centre for Geosciences, Potsdam, Germany<sup>b</sup>UFZ Helmholtz Centre for Environmental Research, Leipzig, Germany

---

### Abstract

A numerical scheme coupling TOUGH2 and the hydro-mechanical simulator OpenGeoSys is used to evaluate the deformations and in situ stress changes induced by CO<sub>2</sub> injection at a potential storage site located in the Northeast German Basin (NEGB). Scenario analysis shows that under the given assumptions the vertical displacement of the reservoir is negligible and significant changes in the recent stress field are limited to the surrounding of the injection well. The undertaken assessment is generally representative for CO<sub>2</sub> storage in the NEGB. However, simulation results suggest that a larger modeling area needs to be considered to avoid boundary effects.

© 2013 The Authors. Published by Elsevier Ltd.

Selection and/or peer-review under responsibility of the GFZ German Research Centre for Geosciences

*Keywords:* CO<sub>2</sub> storage; hydro-mechanical coupling; faults; displacement; stress field

---

### 1. Introduction

Carbon dioxide (CO<sub>2</sub>) storage in deep saline aquifers is one of the Carbon Capture and Storage (CCS) options suggested to reduce greenhouse gas emissions into the atmosphere [1]. However, the stress alterations due to related pore pressure changes during the injection process may lead to severe drawbacks such as ground uplift, reservoir and caprock fracturing, fault reactivation as well as brine migration or

---

\* Corresponding author. Tel.: +49-331-288-28723; fax: +49 331 288-1529.

E-mail address: [fabienma@gfz-potsdam.de](mailto:fabienma@gfz-potsdam.de)

leakage [2]. As a consequence, interest in simulating these phenomena has grown. The numerical studies of hydro-mechanical processes require solving mass and momentum balance equations of fluid and solid phases [3]. In sedimentary basin, this is particularly challenging because of the strong heterogeneities of both structural and physical properties of the formation units. Until now, only a few failure analyses due to CO<sub>2</sub> injection at basin-scale have been conducted numerically, e.g. [4-5].

In the present study, numerical simulations of coupled pore pressure and stress are used to investigate the hydro-mechanical behaviour of a prospective CO<sub>2</sub> storage site in the NEGB with regard to stress changes. Transient distribution of pore pressure calculated with TOUGH2-MP/ECO2N [6] as discussed by Tillner et al. [8] are used in coupled hydro-mechanical equations solved with the scientific software package OpenGeoSys (OGS) [7]. First, the geological site and the numerical scheme involving both software packages are briefly described. Then, the numerical results are illustrated with particular emphasis on vertical displacements. Finally, the modelled hydro-mechanical effects are analysed in terms of a failure analysis. The presented results illustrate a site-specific study-case of hydro-mechanical effects in a well-constrained 3D geological basin based on characterization of residual rocks, and can therefore be representative for CO<sub>2</sub> storage in the Middle Bunter sandstones of the NEGB.

## 2. Study area

The study area Beeskow-Birkholz is located in the NEGB, approximately 80 km southeast of Berlin. It is part of a Mesozoic anticline structure overlaying an Upper Permian (Zechstein) salt dome (Fig. 1). A thorough description of the study area is given by Tillner et al. [8] and Röhmann et al. [9], and therefore omitted here.

The 3D geological model used for the numerical simulations extends over an area of about 40 km x 40 km and includes the major northwest striking fault zones (Guben-Fuerstenwalde and Lausitzer Abbruch fault systems) in a simplified configuration of four discrete faulted areas (Fig. 1). The Detfurth Formation of the Middle Bunter is about 23 m thick and considered as a potential storage reservoir. The sequence is characterized by a multi-barrier system of caprocks of the Upper Bunter, the Middle and Upper Muschelkalk with proven sealing capabilities. In total, the model consists of seven formations from the Stuttgart Formation to the bottom of the Detfurth Formation. Two additional units acting as the top at a depth of 300 m (not displayed in Fig. 1) and the basement at 2200 m depth are added in order to apply the boundary conditions for the numerical simulations to be carried out.

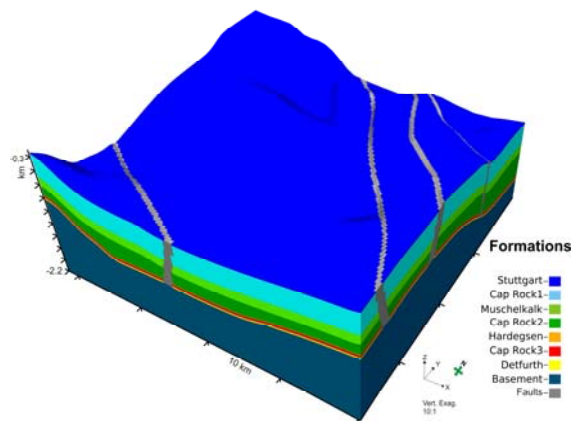


Fig. 1. 3D geological model implemented in the hydro-mechanical simulator OGS. The potential storage reservoir is the Detfurth Formation

### 3. Numerical approach

Here, a one-way coupled approach is used to simulate coupled hydro-mechanical processes as described by Vidal-Gilbert et al. [4] and Rutqvist et al. [10]. The continuity equations for fluid flow are first solved by assuming a non-deformable body. The pressure distribution obtained is then used to solve the mechanical equilibrium equations for stress and strain. The PETREL software package [11] serves as data exchange tool to store a common mesh for both simulators, as well as hydraulic and physical rock properties. The following chart summarizes the workflow applied.

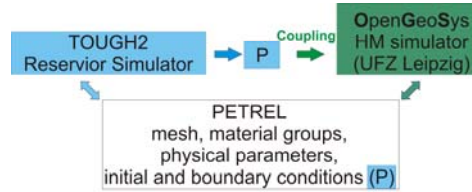


Fig. 2. Chart illustrating the one-way coupling approach used in this study. Pore pressure derived from the simulator TOUGH2 is used as input for the hydro-mechanical simulator OGS. Physical parameters, properties and mesh are transferred using the PETREL software package

The governing equations solved by OGS combine the mass balance equations and the momentum balance equation of fluid and solid phases according to Lewis et al. [12]. The deformation process is solved with respect to the unknowns  $p$  (pressure) and  $u$  (solid displacement) by the system:

$$\nabla \cdot (\boldsymbol{\sigma}' - p\mathbf{I}) + \rho\mathbf{g} = \mathbf{0} \tag{1}$$

$$\boldsymbol{\sigma}' - \mathbf{C}\boldsymbol{\varepsilon}(\mathbf{u}) = \mathbf{0} \tag{2}$$

where  $\boldsymbol{\sigma}'$  denotes the effective stress determined by the difference of total stress and pore pressure, and the momentum balance equation is modified such that it incorporates stresses and forces connected to the fluid pressure.  $\mathbf{I}$ ,  $\mathbf{g}$  and  $\mathbf{C}$  are the identity vector, the gravity vector and the elasticity tensor, respectively.  $\rho\mathbf{g}$  is the volume force with the bulk density defined as  $\rho = \rho^s(1 - \phi) + \rho^l\phi$ , where  $\phi$  is the porosity and  $l, s$  superscripts denote pore fluid and solid phase, respectively. Linear elasticity is assumed, and hence elastic strain  $\boldsymbol{\varepsilon}$  is directly proportional to the effective stress  $\boldsymbol{\sigma}'$  according to the well-known Hooke's law [13]. Fluid flow in deformable porous media is described by the following mass and momentum balance equations,

$$S \frac{\partial p}{\partial t} + \nabla \cdot (\mathbf{w}) + \nabla \cdot \left( \frac{\partial \mathbf{u}}{\partial t} \right) = 0 \tag{3}$$

$$\mathbf{w} + \frac{\mathbf{k}}{\mu} (\nabla p - \rho^l \mathbf{g}) = \mathbf{0} \tag{4}$$

The fluid mass balance Equation 3 has an extra term due to the deformation process. Equation 4 is known as the Darcy law where  $w$  is the volumetric flux of the fluid,  $\mathbf{k}$  is the permeability tensor,  $\mu$  is the fluid dynamic viscosity.  $S$  is the specific storage which is assumed to be independent of the pressure.

Benchmark test cases validating OGS against the commercial mechanical simulator ABAQUS [14] are discussed in [15].

### 3.1. Mesh

The mesh implemented using the Petrel software package consists of almost a million hexahedral elements with a spatial resolution of 250 m in the horizontal plane and variable vertical resolution (Fig. 3). By example, the highly permeable Detfurth storage formation is subdivided into ten layers with a resolution of 2.5 m.

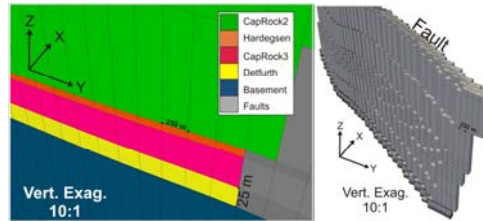


Fig. 3. Example of hexahedral mesh used in the present study

Fault zones can be represented by surface interfaces, equivalent continuum using solid elements or by a combination of both [16]. Because of the numerical requirements of OGS, the equivalent porous media representation by solid elements is chosen. The final mesh is converted from the Petrel software package to an OGS compatible format ensuring the hydro-mechanical simulations to be stable and efficient.

### 3.2. Physical properties

The following hydraulic and elastic properties are assigned to each formation of the model and are adapted from Tillner et al. [8] referring to the “open fault” scenario discussed therein, i.e. the faults act as conduit for fluid flow. The elastic properties of the main aquifers are derived from Ouellet et al. [17], Nagelhout et al. [18], Klapperer et al. [19], Reyer et al. [20] whereas those of the caprocks are inferred from the NAGRA [21] and NER [22] technical reports.

Table 1. Hydraulic and elastic properties assigned to each formation of the hydro-mechanical model [17-21]

Formations	Hydraulic permeability $k$ ( $m^2$ )	Porosity $\phi$	Young's modulus $E$ (GPa)			Poisson Ratio $\nu$	Density $\rho^s$ ( $kg/m^3$ )
			Mod1	Mod2	Mod3		
Top	$10^{-16}$	0.2	4	6	9	0.2	2,600
Stuttgart	$10^{-13}$	0.25	2	4	5	0.2	2,500
Cap Rock 1	$10^{-20}$	0.01	3	6	8	0.27	2,600
Muschelkalk	$2 \times 10^{-13}$	0.2	27	33	45	0.25	2,400
Cap Rock 2	$10^{-20}$	0.01	6	8	11	0.27	2,670
Hardeggen	$3 \times 10^{-13}$	0.16	25	27	30	0.29	2,100
Cap Rock 3	$10^{-20}$	0.01	5	7	9	0.27	2,670
Detfurth	$4 \times 10^{-13}$	0.17	20	23	25	0.29	2,200
Basement	$10^{-20}$	$10^{-5}$	60	60	60	0.3	2,800
Faults	$10^{-12}$	0.17	2	23	30	0.29	2,100

Three different values of the Young's Modulus (Mod1, Mod2, Mod3) are assigned to each formation in the sensitivity analysis representing average values at basin-scale which allow a vertical differentiation of the major formations with respect to hydraulic and mechanical properties.

### 3.3. Boundary and initial conditions

At the model top (-300 m), a constant load and pore pressure are applied, whereas nil displacement is set orthogonal to each lateral side of the model. The pore pressure of the whole system derived from Tillner et al. [8], whereby 1.7 Mt CO<sub>2</sub> per year is injected into the Detfurth Formation. The one-way coupling with the hydro-mechanical simulator OGS is realized for four time steps (10 days, 1 year, 10 years and 20 years) by integrating the calculated pore pressures (Fig. 4) as Dirichlet boundary into the hydro-mechanical model, as illustrated in Fig. 2.

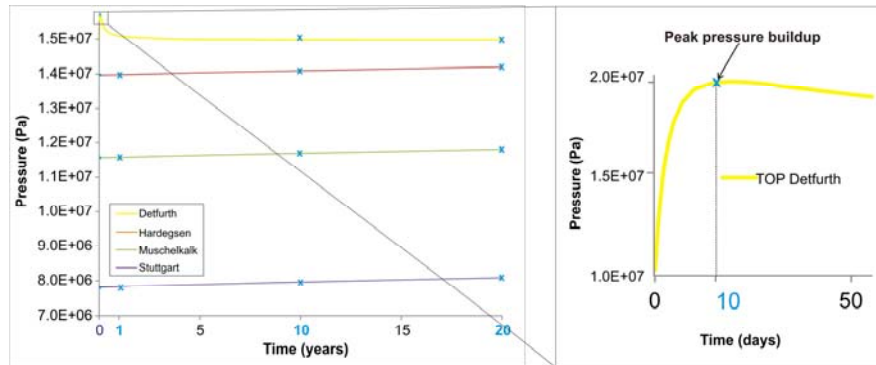


Fig. 4. Average pore pressure trends [8] over the injection period. Four time steps are selected (10 days, 1 year, 10 years and 20 years) as boundary conditions for the hydro-mechanical simulations

The peak pore pressure at the Detfurth Formation is observed after 10 days to 20 days of injection. In the overlying aquifers, pore pressure increases linearly of approximately 0.5 MPa over the whole injection period due to the hydraulically conductive faults. The initial pressure conditions are derived from a steady groundwater state simulations and an equilibrium stress field initializes each hydro-mechanical simulation.

## 4. Results

Stress changes and vertical displacements for the scenario “Mod3” (Table 1) are illustrated in Fig. 6. During CO<sub>2</sub> injection, the effective stress variations are mainly induced by pore pressure changes in the aquifers. However, the strong mechanical and structural heterogeneities of the formations also play a role in determining the final state of both stress and displacement, as found in Vidal-Gilbert [4]. After 10 days of injection, ground uplift can be observed in a radius of 1.8 km around the injection point (Fig. 5): the maximum vertical displacement at the top of the Detfurth Formation is 9 mm and 4 mm at the top of the Stuttgart Formation. After 20 years of CO<sub>2</sub> injection, the maximum vertical displacement of the top of the Stuttgart Formation is 14 mm, i.e. 3 mm higher compared to that at the top of the Detfurth Formation (Fig. 5). The more pronounced displacement of the upper aquifer is due to the fact that increase of pore pressure is not only limited to the Detfurth Formation but also affects the overlying sediments due to the hydraulic conductivity of the present faults (Fig. 4). This causes a surface displacement of 10 mm in the

areas between the faults which, in this scenario, act as stiff bounding walls. To further investigate this effect, we ran a simulation in which the pore pressure increases only in the Defurth Formation. By doing so, it turned out that the maximum vertical displacement of the top of the Detfurth Formation is 9 mm (not displayed in Fig. 6), i.e. 5 mm less than in the previous case, and only 1 mm displacement occurs in between the faults.

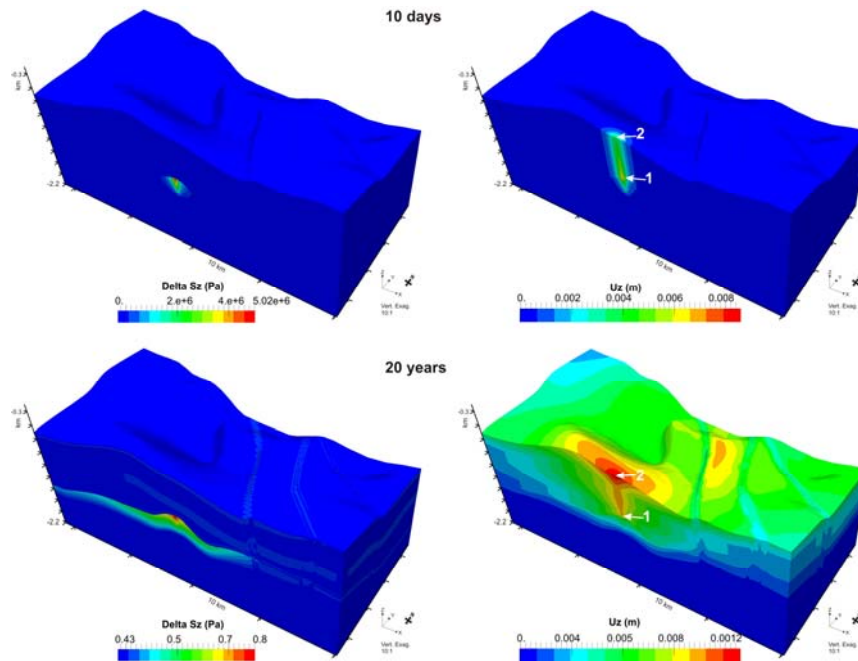


Fig. 5. Scenario Mod3: 3D cross-sections of effective stress changes ( $\Delta Sz$ ) and vertical displacement ( $Uz$ ) after 10 days and 20 years of  $CO_2$  injection.  $Uz$  is plotted over the entire injection period at two observation points (indicated by arrows) in Fig. 6

This simulation findings highlight the importance of implementing the formations surrounding the target reservoir into the hydro-mechanical model to account for the cumulative impacts of pore pressure on effective stress field and ground displacement. The displacement features described above are reflected in all model scenarios (Fig. 6).

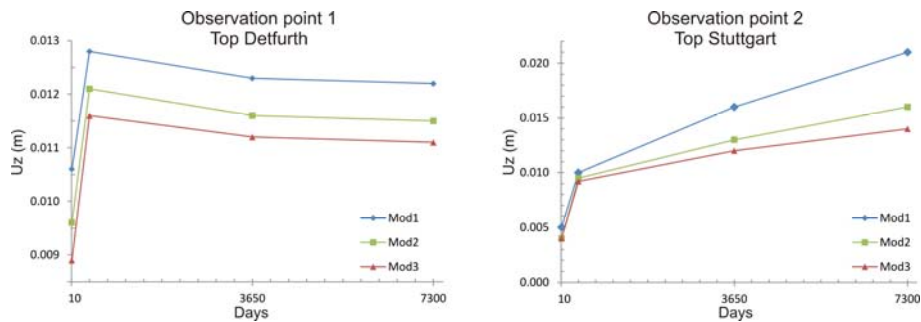


Fig. 6. Vertical displacement trends at two observation points addressed in Fig. 5

However, in the Mod1 scenario, it turns out that the faults undergo the highest vertical displacement because of their relatively low Young’s modulus with respect to the surrounding sediments (Table 1).

As a final analysis, the Mohr-Coulomb (MC) criterion [23] is applied to infer failure conditions of the storage aquifer and surrounding units. Failure occurs if the maximum shear stress  $\tau_m = 1/2(\sigma'_1 - \sigma'_3)$  becomes:

$$f = \frac{|\tau_m|}{C_0 \cos \theta + \sigma'_m \sin \theta} \geq 1 \tag{5}$$

where  $\sigma'_m = 1/2(\sigma'_1 + \sigma'_3)$   $\tau_m = 1/2(\sigma'_1 - \sigma'_3)$  is the mean stress.  $\sigma'_1$  and  $\sigma'_3$  are maximum and minimum principle stress, respectively, i.e. the eigenvalues of the effective stress tensor  $\sigma'$ .  $C_0$  is the cohesion, and  $\theta$  is the internal angle of friction. The failure properties of sandstone were assumed to be  $C_0 = 5$  MPa and  $\theta = 30^\circ$  according to NER [20]. The resulting failure factor is below one (Fig. 7), indicating that the development of shear stress is not critical for the stability of the reservoir formations. However local artifacts develop at the intersection between faults and the model boundaries, suggesting that a larger study area needs to be modeled, as undertaken in the present issue by Roehmann et al [9].

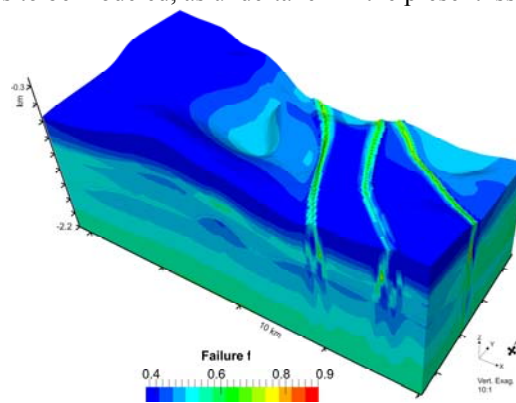


Fig. 7. Failure factor  $f$ (Equation 5) of the scenario Mod3, calculated with  $C_0 = 5$  MPa and  $\theta = 30^\circ$

The effective stress path within the Detfurth Formation is plotted on a Mohr diagram (Fig. 8).  $\text{CO}_2$  injection induces a decrease of both effective and shear stress in the reservoir. Furthermore, despite its shift, the stress path still lays below the estimated sandstone failure line. Assuming an unrealistic cohesionless sandstone, failure would occur for friction angles below  $28^\circ$  (Fig. 8).

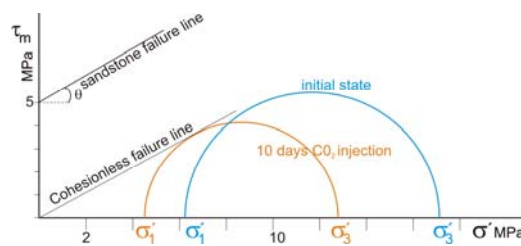


Fig. 8. Mohr-Coulomb representation of the effective stress path within the Detfurth Formation after 10 days of  $\text{CO}_2$  injection. The Mohr-Coulomb failure line for the sandstone is determined by a cohesion of 5 MPa and a friction angle of  $30^\circ$

## 5. Conclusions

A one-way coupling between the hydro-mechanical simulator OGS and the multi-phase simulator TOUGH2 was implemented in order to investigate the mechanical changes induced by CO<sub>2</sub> injection into a storage formation of the NEGB. Given the hydraulic and elastic properties investigated in three simulation scenarios, failure analysis indicates that effective stress changes induced by pore pressure variations do not induce any shear failure in the reservoir or its caprocks. Our simulations show that ground displacement is determined by the cumulative effects of pore pressure increase in the aquifers overlying the Detfurth Formation. As a result, sediments uplift can be higher at the top of the Stuttgart Formation than at the top of the Detfurth Formation. The structural and physical heterogeneities of the system also play a role in determining the resulting mechanical state of the entire geologic system. If faulted areas are implemented as highly consolidated sandstones (Mod3), ground surface can experience upward vertical displacements between the rigid faults. By contrast, major displacements will occur along the faults, if these are less stiff than the surrounding sediments (Mod1). In that respect, the sensitivity analysis suggests that a larger study area needs to be modeled in order to rule out boundary effects at the side walls where nil displacement is imposed. A supra-regional scale hydro-mechanical model of the study area is discussed by Roehmann et al. [9] in the present issue.

## Acknowledgements

We gratefully acknowledge the funding support from the German Federal Ministry of Education and research (grant 03G0758A/B) in the frame of the R&D program GEOTECHNOLOGIEN, publication GEOTECH-2100.

## References

- [1] Lackner KS. Climate change. A guide to CO<sub>2</sub> sequestration. *Science* 2003;**300**:1677-1678.
- [2] Rutqvist J. The geomechanics of CO<sub>2</sub> storage in deep sedimentary formations. *Geotech Geol Eng* 2012;**30**:525–551.
- [3] Wang W, Kolditz O. Object-oriented finite element analysis of thermo-hydro-mechanical (THM) problems in porous media. *Int J Numer Methods Eng* 2007;**69**:162-201.
- [4] Vidal-Gilbert S, Nauroy JF, Brosse E. 3D geomechanical modelling for CO<sub>2</sub> geologic storage in the Dogger carbonates of the Paris Basin. *Int J Greenhouse Gas Control* 2009;**3**:288-299.
- [5] Cappa F, Rutqvist J. Modeling of coupled deformation and permeability evolution during fault reactivation induced by deep underground injection of CO<sub>2</sub>. *International Journal of Greenhouse Gas Control* 2011;**5**:336–346.
- [6] Zhang K, Wu YS, Pruess K. User's Guide for TOUGH2-MP – A Massively Parallel Version of the TOUGH2 Code. Report LBNL-315E, Earth Sciences Division, Lawrence Berkeley National Laboratory, Berkeley, California, 2008. [7] Wang W, Kosakowski G, Kolditz O. A parallel finite element scheme for thermo-hydro-mechanical (THM) coupled problems in porous media. *Comput Geosci* 2009;**35**:1631–1641.
- [8] Tillner E, Kempka T, Nakaten B, Kühn M. Brine migration through fault zones: 3D numerical simulations for a prospective CO<sub>2</sub> storage site in Northeast Germany. *Int J Greenhouse Gas Control* 2013 (in press) <http://dx.doi.org/10.1016/j.ijggc.2013.03.012>.
- [9] Röhm L, Tillner E, Magri F, Kühn M, Kempka T. Fault reactivation and ground surface uplift assessment at a prospective German CO<sub>2</sub> storage site. *Energy Procedia* 2013. this issue.
- [10] Rutqvist J, Wu YS, Tsang CF, Bodvarsson G. A modelling approach for analysis of coupled multi-phase fluid-flow, heat transfer, and deformation in fractured porous rock. *Int. J. Rock Mech. Mining Sci* 2002;**39**:429–442.
- [11] Schlumberger. Petrel Seismic-to-Evaluation Software, Version 2010.2.2.



- [12] Lewis RW, Roberts PJ, Schrefler BA. Finite element modelling of two-phase heat and fluid flow in deforming porous media. *Transport in Porous Media* 1989;4:319–334.
- [13] Jaeger, JC, Cook, NGW, Zimmerman, RW. *Fundamentals of rock mechanics*. 4th Ed. John Wiley & Sons; 2007.
- [14] Abaqus FEA,D S Simulia. Dassault Systèmes, 2004, 2007.
- [15] Magri F, Kempka T, Tillner E, Zimmerman G. In: Kolditz O, Görke UJ, Shao H, Wang W, Editors. *Thermo-Hydro-Mechanical-Chemical Processes in Porous Media*, Berlin- Heidelberg-New York: Springer-Verlag; in print, Chapter 2 Consolidation (HnM) processes.
- [16] Rutqvist J, Cappa F, Birkholzer, J, Tsang CF. Estimating maximum sustainable injection pressure during geological sequestration of CO<sub>2</sub> using coupled fluid flow and geomechanical fault-slip analysis. *Energy Conversion and Management* 2007;48:1798–1807.
- [17] Ouellet A, Bérard T, Frykman P, Welsh P, Minton J, Pamucku Y, Hurter S, Schmidt-Hattenberger C. Reservoir geomechanics case study of seal integrity under CO<sub>2</sub> storage conditions at Ketzin, Germany. Ninth Annual Conference on Carbon Capture and Sequestration May 10-13, 2010.
- [18] Nagelhout, ACG and Roest, JPA. Investigating fault slip in a model of an underground gas storage facility. *Int J Rock Mech & Min Sci* 1997;34(3-4):Paper No. 212.
- [19] Klapperer S, Moeck I, Norden, B, Backers, T. Geomechanical characterization of an Upper Triassic reservoir rock (Stuttgart Formation) in the NE German Basin (pilot site for CO<sub>2</sub> storage at Ketzin, Germany). EGU General Assembly (Vienna, Austria), *Geophysical Research Abstracts* 2012;14:2051.
- [20] Reyer D, Philipp SL. Heterogeneities of mechanical properties in potential geothermal reservoir rocks of the North German Basin. EGU General Assembly (Vienna, Austria), *Geophysical Research Abstracts* 2012;14:346.
- [21] NER Modulus dispersion in sandstone and limestone. New England Research, Inc; 2001.
- [22] NAGRA Technischer Bericht 00-01 Sondierbohrung Benken Untersuchungsbericht; August 2001.
- [23] Labuz J, Zang A. Mohr-Coulomb Failure Criterion. *Rock Mechanics and Rock Engineering* 2012; 45:975 - 979.